

Theoretical studies of the mechanism of the action of the neurohypophyseal hormones. I. Molecular electrostatic potential (MEP) and molecular electrostatic field (MEF) maps of some vasopressin analogues

Adam Liwo, Anna Tempczyk and Zbigniew Grzonka*

Institute of Chemistry, University of Gdańsk, ul. Sobieskiego 18, 80952 Gdańsk, Poland

Received 17 January 1989

Accepted 17 March 1989

Key words: Vasopressin analogues; Molecular electrostatic potential; Molecular electrostatic field; Recognition binding; Biological activity

SUMMARY

Continuing our theoretical studies of the oxytocin and vasopressin analogues, we have analysed the molecular electrostatic potential (MEP) and the norm of the molecular electrostatic field (MEF) of [1- β -mercapto- α -propionic acid]-arginine-vasopressin ([Mpa¹]-AVP), [1-(β -mercapto- β , β -cyclopentamethylene)propionic acid]-arginine-vasopressin ([Cpp¹]-AVP), and [1-thiosalicylic acid]-arginine-vasopressin ([Ths¹]-AVP) whose low-energy conformations were calculated in our previous work. These compounds are known from experiment to exhibit different biological activity. The scalar fields mentioned determine the energy of interaction with either charged (MEP) or polar (MEF) species, the energy being in the second case either optimal or Boltzmann-averaged over all the possible orientations of the dipole moment versus the electrostatic field. The electrostatic interactions slowly vanish with distance and can therefore be considered to be the factor determining the molecular shape at greater distances, which can help in both predicting the interactions with the receptor at the stage of remote recognition and in finding the preferred directions of solvation by a polar solvent. In the analysis of the fields three techniques have been used: (i) the construction of maps in certain planes; (ii) the construction of maps on spheres centered in the charge center of the molecule under study and of poles chosen according to the main axes of the quadrupole moment; and (iii) the construction of surfaces corresponding to a given value of potential. The results obtained show that the shapes of both MEP and MEF are similar in the case of [Mpa¹]-AVP and [Cpp¹]-AVP (biologically active), while some differences emerge when comparing these compounds with [Ths¹]-AVP (inactive). It has also been found that both MEP and MEF depend even more strongly on conformation.

*To whom correspondence should be addressed.

INTRODUCTION

Studies of the interactions of biologically active compounds with other systems and with the environment are very important in investigating the mechanism of their biological action. In the case of hormones or neurotransmitters it is essential to obtain some knowledge of their ability in particular interactions with the receptors, interactions which in turn consist of three steps: *recognition-binding*, the *chemical reaction* which is itself, or induces, the biological response, and the *reversal* which restores the biomolecule [1,2].

In the case of neurohypophyseal hormones, in contrast to that of enzymes, no detailed 'chemical' mechanism of their action has been established as yet. One reason for this is the complexity of the receptors, which consist of several protein and lipid shells, making it difficult to locate the active sites. Moreover, such a structure is very labile and breaks even on isolating the receptor from the plasma membrane or from cytosol, which makes investigation of it by ordinary physico-chemical methods impossible [3]. Another obstacle is the complexity of the biological response itself, as it, in turn, consists of several stages, some of which are still unknown. However, based on the analogues known from experiment to exhibit either agonistic or antagonistic activity, or to be inactive, some conclusions concerning the receptor can be drawn [3,4].

The fundamental factor which must be taken into account when attempting to theoretically investigate the biological activity is the conformational space of the compounds under study. So far, many approaches have been developed in which either the lowest energy conformations of various analogues are compared [5,6] or the conformational space is investigated more thoroughly by means of Monte Carlo or molecular dynamics methods [7,8]. This is a very difficult task because, in general, the peptide hormones are rather flexible molecules of a size sufficient to assume thousands of low-energy conformations, the barriers between which are relatively low.

It must also be borne in mind that the polar environment, which in the case of living systems is water, very often remarkably changes the conformational space allowed for a biomolecule [9]. Therefore, various solvation models have been developed [9], for example that of Némethy et al. [10] which makes it possible to take into account the solvation effects already in the geometry optimisation. On the other hand, for many force fields used in the conformational calculations on peptides and other compounds of biological significance, the effect of solvation is included implicitly both in the expression for the steric energy and in the parameters [9,11].

Having established the conformational space of a given hormone, we can raise the question of its interactions with the receptor. For the reasons presented above, an immediate answer is impossible. However, owing to the fact that if their mutual distance is large enough, both hormone and receptor remain almost unperturbed, we can estimate the sites of the hormone where certain types of interactions are particularly strong, or particularly weak. This accounts for the first phase of the recognition-binding stage which is sometimes called *remote recognition* [12].

In general, the long-range interactions can be either of the electrostatic (in the classical sense) or of the dispersion type. Depending on the assumed type of the active site of the receptor (hydrophobic or hydrophilic) we can calculate various quantities characterising such interactions. For example, an approach has been developed in which the interaction energy with a test probe (proton, water, or methyl group), or its differences between various analogues, are integrated over all the space available and used as parameters in QSAR [13]. A more justified approach, however, is the one in which the spatial distribution of the interaction energy field is considered. If, for exam-

ple, a surface is calculated on which this energy is equal to a certain threshold value, this surface can be considered to be a *molecular surface* and its topographic features can help in matching the appropriate structure of the receptor. Such surfaces were constructed both in the hard-sphere approximation [14] and by comparing the energy of interaction with the probe species (water, ammonium ion, and the methyl group) [15,16]. Investigating their topographic properties, in particular such peculiarities as the bumps and holes, appears promising [14].

In our recent paper [17], we calculated low-energy conformations of some vasopressin analogues substituted in position 1, namely [1β -mercaptopropionic acid]-arginine-vasopressin ($[Mpa^1]\text{-AVP}$), [1β -mercapto- β,β -cyclopentamethylene]propionic acid]-arginine-vasopressin ($[Cpp^1]\text{-AVP}$), and [1 -thiosalicylic acid]-arginine-vasopressin ($[Ths^1]\text{-AVP}$). The primary structures of these compounds and of their parent hormone are shown in Fig. 1.

The analogues under consideration differ substantially in their biological activity. [Mpa^1]-AVP is a full agonist of both the antidiuretic and the pressor response [18], while [Cpp^1]-AVP is an antagonist of the vasopressor response, which is also reflected in the fact that it has, similar to vasopressin, affinity to the V_1 and much lower to the V_2 vasopressor receptor [19,20]. In contrast, [Ths^1]-AVP is a very weak agonist of the antidiuretic and pressor responses [21] and its affinity to both the V_1 and the V_2 receptors is very low. This is in agreement with the results of our conformational calculations, as the lowest energy conformations of [Mpa^1]-AVP and [Cpp^1]-AVP are almost identical, except for the presence of a cyclohexane ring which may be the factor inhibiting the biological response and the sterical hindrance making the binding to the V_2 receptor difficult. In contrast, the lowest energy conformation of [Ths^1]-AVP differs more [17].

In this work we consider the molecular electrostatic fields of the compounds mentioned, assuming the conformations previously found. Such fields determine the electrostatic interactions involving a given molecule. On the other hand, it is well known that the energy of interactions which

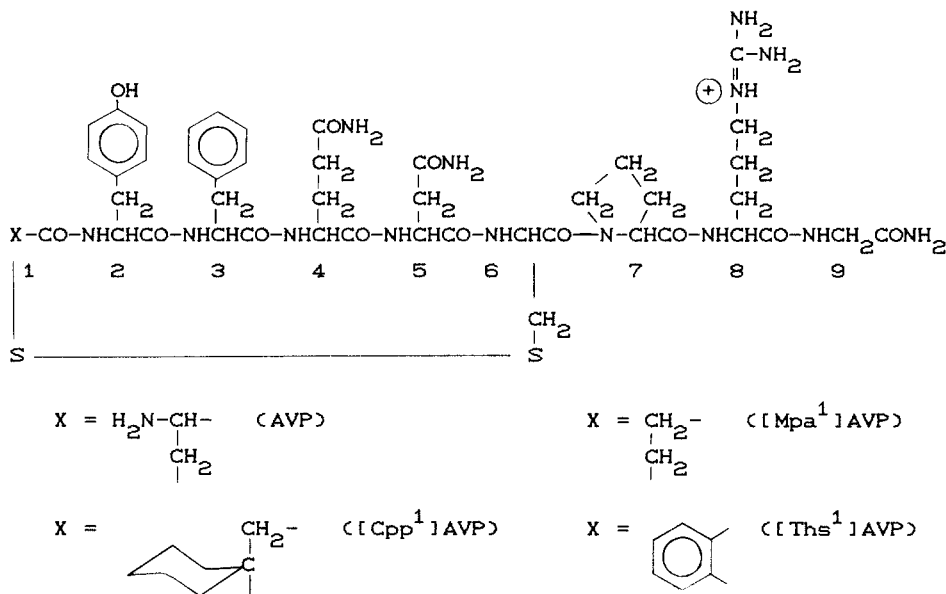


Fig. 1. Primary structure of arginine-vasopressin (AVP) and its analogues studied in this work.

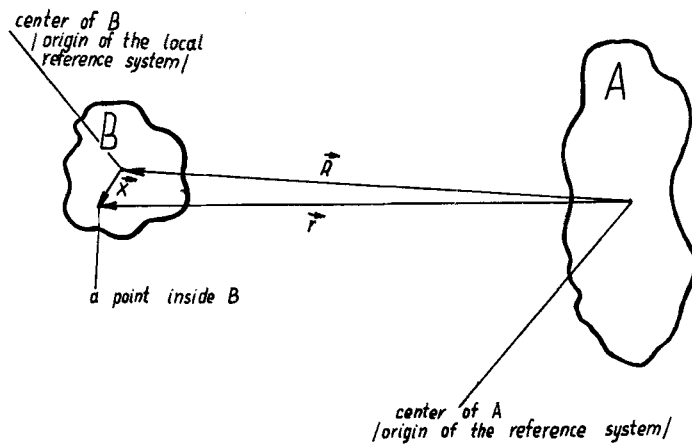


Fig. 2. Definition of the parameters of mutual orientation of the hormone molecule (system A) and the interacting system (B).

involve the polar groups, for example those leading to the formation of hydrogen bonds, can be approximated with considerable accuracy, even at small distances, by the electrostatic contribution [22]. The electrostatic interactions vanish slowly with distance and can therefore be considered to be the factor determining the long-range interactions both with the environment and with the receptors. In the latter case, the electrostatic field can be interpreted as the shape of a hormone which is to be 'seen' by the receptor. It is therefore very important whether the molecular electrostatic fields of [Ths¹]-AVP substantially differ from those of [Mpa¹]-AVP and [Cpp¹]-AVP, which would explain the lack of any considerable activity of the first analogue.

The following papers in this series are to be devoted to other types of interaction, as well as to deducing the structure of the receptor and the mechanism of the biological response.

THEORY

Let us consider the electrostatic interactions of the hormone under study, henceforth denoted by A, with another system, denoted by B. System B can be the solvent molecule, the active site of a receptor, etc. Let the reference system be chosen as shown in Fig. 2.

As can be seen, the origin of the system is a point inside A, for example its charge center, and \mathbf{r} denotes the position vector of a point inside B. Because the distance between the centers of A and B is assumed to be comparatively large, it is convenient to express \mathbf{r} as a sum of \mathbf{R} , the position vector of the center of B and \mathbf{x} the position vector of the point with respect to the center of B. If $V(\mathbf{r})$ is the molecular electrostatic potential of system A, and $\rho(\mathbf{r})$ is the charge distribution of system B, the electrostatic energy can be expressed by (1) [23].

$$U(\mathbf{r}; \theta) = \int_{\Omega \subset \mathbb{R}^3} V(\mathbf{R} + \mathbf{x}) \rho(\mathbf{R} + \mathbf{x}) d^3x \quad (1)$$

where Ω is the region occupied by B, and θ stands for the parameters describing the orientation of system B in the global coordinate system, for example three Euler angles.

It should be stressed that, in the expression above, V is that part of the electrostatic potential which is generated only by A. If the functions integrated contained the total charge distribution of systems A and B and the total electrostatic potential, a factor of $\frac{1}{2}$ should appear at the integration sign.

For those values of x such that $\|x\|$ is small when compared with $\|\mathbf{R}\|$ (1) can be expanded into the multipole series (2) [23].

$$U(r; \theta) = qV(\mathbf{R}) + \mathbf{p} \cdot \nabla V(\mathbf{R}) + \frac{1}{3}Q \cdot \nabla \nabla V(\mathbf{R}) + \dots \quad (2)$$

where

$$q = \int_{\Omega \subset \mathbb{R}^3} \rho(x) d^3x \text{ is the net charge of the system} \quad (3)$$

$$\mathbf{p} = \int_{\Omega \subset \mathbb{R}^3} x\rho(x) d^3x \text{ is the dipole moment} \quad (4)$$

$$Q = \frac{1}{2} \int_{\Omega \subset \mathbb{R}^3} 3\rho(x) (xx - \frac{1}{3}\|x\|\delta_{xx}) d^3x \text{ is the quadrupole moment} \quad (5)$$

$$\delta_{xx} \text{ is the Kronecker symbol; } \delta_{xi,xj} = \begin{cases} 1 & \text{for } i = j \\ 0 & \text{for } i \neq j \end{cases}$$

and integration is performed in the local coordinate system so that

$$f(\mathbf{R} + x) \rightarrow f(x).$$

Depending on the problem being investigated, different terms of this expansion can be taken into account.

The first term includes the cases when the system interacting with the biomolecule is charged (protonation, interactions with alkali metal ions, etc.), as the interaction energy at a given point can, in such cases, be estimated by the product of the molecular electrostatic potential of system A and the charge of system B. Other terms which depend on the spatial distribution of the charge of B are not so important, as they vanish much more quickly with the distance. To obtain knowledge of the preferred sites of interaction, usually either the maps of V in certain planes (the so-called '2-D maps') or the surfaces of constant V in three-dimensional space (the so-called '3-D maps' [16]) are constructed and analysed. Since the work of Scrocco and Tomasi [24] it has become a very popular tool for studying acidic-basic properties, the complexing of biomolecules by metal ions [25], and even the correlation of the shapes of the maps with biological activity, which can

help in drug design [26]. Examples can also be found in papers published up to the present where certain features of MEP, such as the positions and/or depth of its minima, are calculated and used as parameters in QSAR [27].

For closed-shell and uncharged systems, the electrostatic part of the energy of interactions is determined by the higher order multipoles.

In the case of interactions with polar systems, the most important is the second term, which includes the permanent dipole moment. The quantitative estimation of the interaction energy can be based on this term and the energy is thus approximated by a scalar product of the molecular electrostatic field vector (E) of the biomolecule and the dipole moment of the interacting system:

$$U(p; R) = - \mathbf{p} \cdot \mathbf{E}(R), \text{ where } \mathbf{E}(R) = - \nabla V(R) \quad (6)$$

The optimal interaction energy is given by (7):

$$U_{\text{opt}}(R) = - \|p\| \|E(R)\| \quad (7)$$

Taking the Boltzmann average over all the mutual orientations of the vectors p and $E(r)$, and neglecting the higher order terms in the McLaurin expansion of $\exp(-U(r)/kT)$, as in the case of the calculation of the polarisability of polar liquids [28], it can easily be shown that the average interaction energy is expressed by (8):

$$\bar{U}(R) = - \frac{1}{3kT} \|p\|^2 \|E(R)\|^2 \quad (8)$$

Both energies thus depend on the value of the norm of the electrostatic field vector. The function $\|E(r)\|$ can therefore be considered to be the *dipole interaction potential*, an analogue of the molecular electrostatic potential and its maps in various surfaces, as the analogues of the molecular electrostatic potential maps. Such maps will further be called the molecular electrostatic field (MEF) maps. They can help in predicting the directions and energies of interactions with small polar molecules at sufficiently large distances (i.e., greater than the van der Waals sphere). In particular, such maps can serve in the rapid estimation of both the directions and the energy of solvation being, in such a case, much more useful than the maps of MEP. Examples can be found in the previously published works of the use of maps of the energy of interactions with the water (or another solvent's) molecule [14,29]. However, the cost of computing the latter can be estimated to be much higher than that of computing the maps of MEF.

METHODS

As has been mentioned, the electrostatic interactions are especially important at greater distances. We have therefore concluded that the point-charge approximation is sufficient to reliably describe the fields under consideration. Moreover, this has been proved by Singh and Kollman [30]. Also, in our previous work [17] we concluded that the 'accurate' potential obtained from the SCF electronic wave function of a molecule plus its core potential is, at distances greater than 4 Å, very well approximated by the point-charge potential, the charges being centered on atoms and fitted by means of a linear least-squares method. Furthermore, the point-charge approximation in most

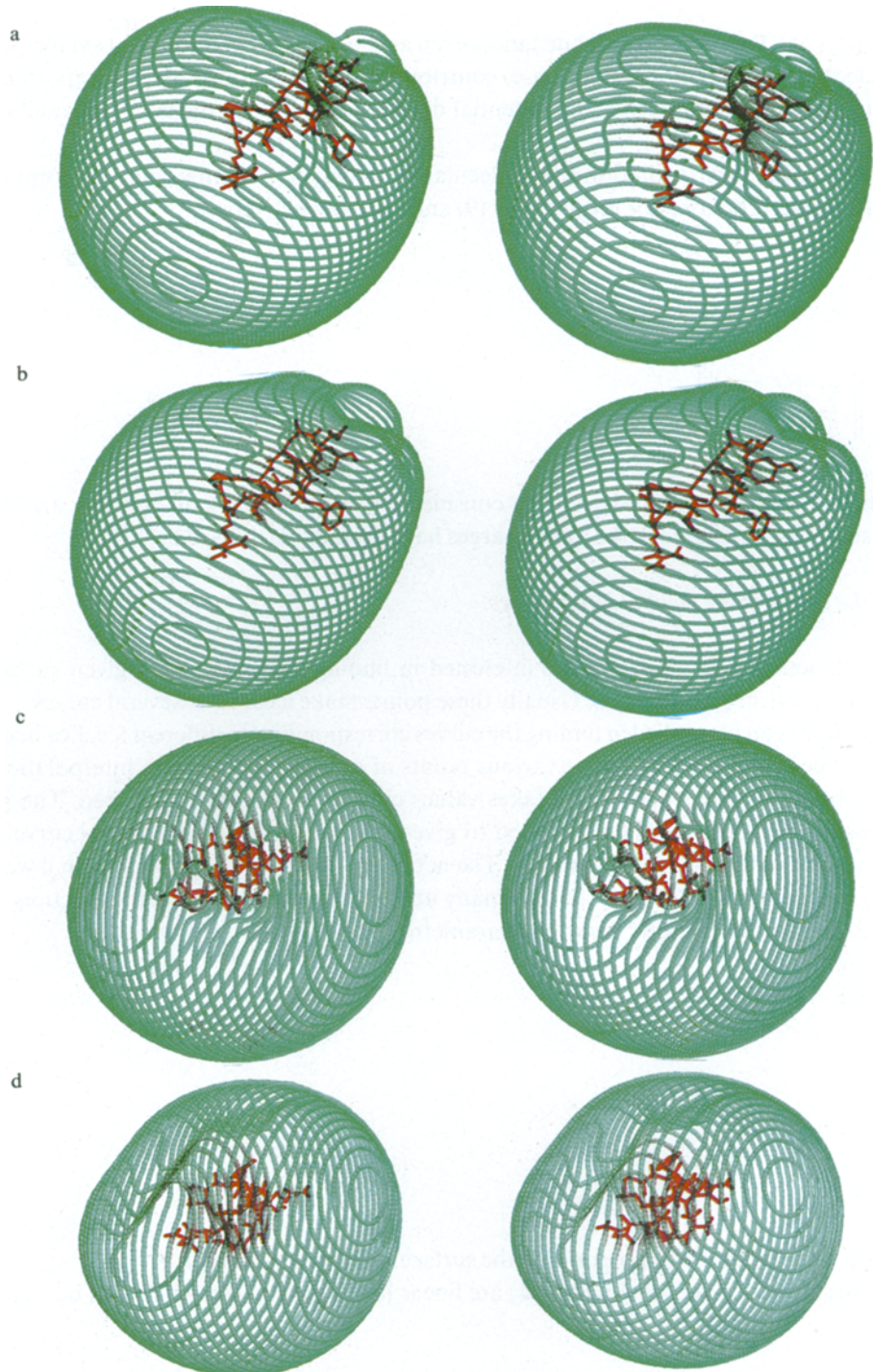


Fig. 3. The 3-D maps of MEP and MEF (green) of two low-energy conformations of $[Mpa^1]\text{-AVP}$ shown together with the molecules (red). The value of MEP of the shapes presented is 20 kcal/mol and that of MEF 1.5 kcal/mol. (a) T_2^- -shaped conformation, MEP; (b) T_2^+ -shaped conformation, MEF; (c) C_1^+ -shaped conformation, MEP; (d) C_1^+ -shaped conformation, MEF.

cases reproduces MEP qualitatively for distances even as short as 2–3 Å. Besides, at smaller distances the nonelectrostatic (in the classical sense) contributions to energy also play an important role and therefore the molecular electrostatic potential does not account for the whole interaction energy.

In the point-charge approximation the molecular electrostatic potential and the norm of the molecular electrostatic field vector are given by (9) and (10), respectively:

$$V(\mathbf{r}) = \sum_{i=1}^n \frac{q_i}{\|\mathbf{r} - \mathbf{r}_i\|} \quad (9)$$

$$\|\mathbf{E}(\mathbf{r})\| = \left\| \sum_{i=1}^n \frac{q_i(\mathbf{r} - \mathbf{r}_i)}{\|\mathbf{r} - \mathbf{r}_i\|^3} \right\| \quad (10)$$

where n is the number of atoms and explicitly considered lone pairs which, in our case, are located only on the sulphurs. In this work the same charges have been taken as used in [17].

Calculating the points of the equipotential curves

Consider a function $f: \mathbf{R}^3 \rightarrow \mathbf{R}$. We are interested in finding the points on a given surface for which f takes an arbitrary value, say f_i . Usually these points make a curve or several curves.

Various methods can be applied in finding the curves corresponding to different f_i 's. For instance, the function values can be calculated at various points of a given net and then interpolation can be performed between points for which f takes values close to one of those required. The points corresponding to a given f_i can then be linked to give an approximate equipotential curve. Such a procedure requires only the function values. The net must, however, be dense enough if we want the curves to be smooth. This involves in turn many unnecessary evaluations of the function.

Let us consider a surface S in \mathbf{R}^3 described parametrically by system (11):

$$\begin{aligned} x &= x(\varphi, \psi) \\ y &= y(\varphi, \psi) \\ z &= z(\varphi, \psi) \end{aligned} \quad (11)$$

or in the vector notation:

$$\mathbf{r} = \mathbf{r}(\varphi, \psi) \quad (11')$$

where φ and ψ are the parameters describing the surface under consideration.

When the surface is a plane, equations (11) are linear in the parameters which can be expressed by (12):

$$\begin{aligned} x &= x^\circ + u_1\varphi + v_1\psi \\ y &= y^\circ + u_2\varphi + v_2\psi \\ z &= z^\circ + u_3\varphi + v_3\psi \end{aligned} \quad (12)$$

or in the vector notation:

$$\mathbf{r} = \mathbf{r}^{\circ} + \varphi \mathbf{u} + \psi \mathbf{v} \quad (12')$$

where $\mathbf{r}^{\circ} = (x^{\circ}, y^{\circ}, z^{\circ})$ is a chosen point lying in the plane, and \mathbf{u} and \mathbf{v} are the vectors spanning the plane. These can always be made orthonormal, so that it can be assumed that $\|\mathbf{u}\| = 1$, $\|\mathbf{v}\| = 1$, and $\mathbf{u} \cdot \mathbf{v} = 0$.

In the case of a sphere the Cartesian coordinates are expressed by (13):

$$\begin{aligned} x &= x^{\circ} + \rho \cos \varphi \sin \psi \\ y &= y^{\circ} + \rho \sin \varphi \sin \psi \\ z &= z^{\circ} + \rho \cos \psi \end{aligned} \quad (13)$$

where $(x^{\circ}, y^{\circ}, z^{\circ})$ is the sphere center, ρ is the radius of the sphere, and φ and ψ are the polar angles. We assume $-\pi < \varphi < \pi$ and $0 < \psi < \pi$.

Consider the system of differential equations given by (14):

$$\begin{aligned} \frac{d\varphi(t)}{dt} &= \delta f(x(\varphi, \psi), y(\varphi, \psi), z(\varphi, \psi)) / \delta \varphi \\ \frac{d\psi(t)}{dt} &= -\delta f(x(\varphi, \psi), y(\varphi, \psi), z(\varphi, \psi)) / \delta \psi \end{aligned} \quad (14)$$

with the initial conditions (14'):

$$\begin{aligned} \varphi(t=0) &= \varphi^{\circ}, \psi(t=0) = \psi^{\circ} \\ f(x(\varphi^{\circ}, \psi^{\circ}), y(\varphi^{\circ}, \psi^{\circ}), z(\varphi^{\circ}, \psi^{\circ})) &\equiv f(\varphi^{\circ}, \psi^{\circ}) = f_i \end{aligned} \quad (14')$$

For each (φ, ψ) being the solution of the system above, we have $f(\varphi, \psi) = f_i$. This can be proved at once, because at each point the direction of the curve is perpendicular to the projection of ∇f onto the surface under consideration.

In practice, to solve system (14) we must apply a discretisation method. Usually the increment in t , Δt , is assigned a constant value. It is also convenient, if the distances between the subsequent points of a curve in the (φ, ψ) space are equal. However, when solving system (14) taking a constant value of Δt , these distances are proportional to the norm of the vector of derivatives $(\delta f / \delta \varphi, \delta f / \delta \psi)$. Therefore, instead of (14) we solved its modified version (15), which has the same solution and for which the equidistance condition holds:

$$\begin{aligned} \delta \varphi(t) / \delta t &= [(\delta f / \delta \varphi)^2 + (\delta f / \delta \psi)^2]^{-\frac{1}{2}} \delta f / \delta \varphi \\ \delta \psi(t) / \delta t &= -[(\delta f / \delta \varphi)^2 + (\delta f / \delta \psi)^2]^{-\frac{1}{2}} \delta f / \delta \psi \end{aligned} \quad (15)$$

with the initial conditions (14').

The derivatives in φ and ψ can easily be expressed in terms of the derivatives in the Cartesian coordinates:

$$\begin{aligned} \delta f / \delta \varphi &= \delta f / \delta x \delta x / \delta \varphi + \delta f / \delta y \delta y / \delta \varphi + \delta f / \delta z \delta z / \delta \varphi \\ \delta f / \delta \psi &= \delta f / \delta x \delta x / \delta \psi + \delta f / \delta y \delta y / \delta \psi + \delta f / \delta z \delta z / \delta \psi \end{aligned} \quad (16)$$

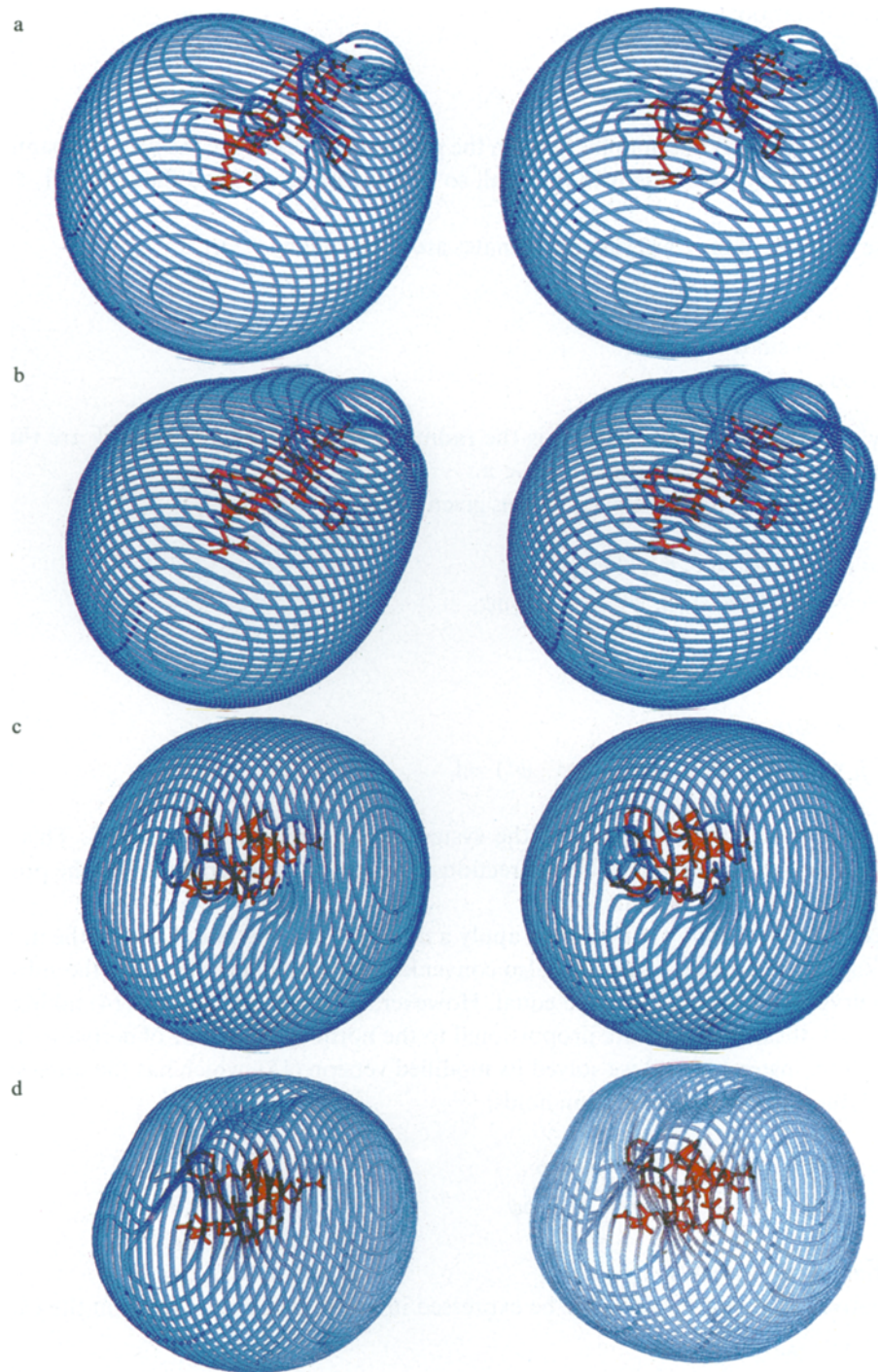


Fig. 4. The 3-D maps of MEP and MEF (blue) of two low-energy conformations of $[Cpp^1]$ -AVP shown together with the molecules (red). The value of MEP of the shapes presented is 20 kcal/mol and that of MEF 1.5 kcal/mol. Parts (a)–(d) as in Fig. 3.

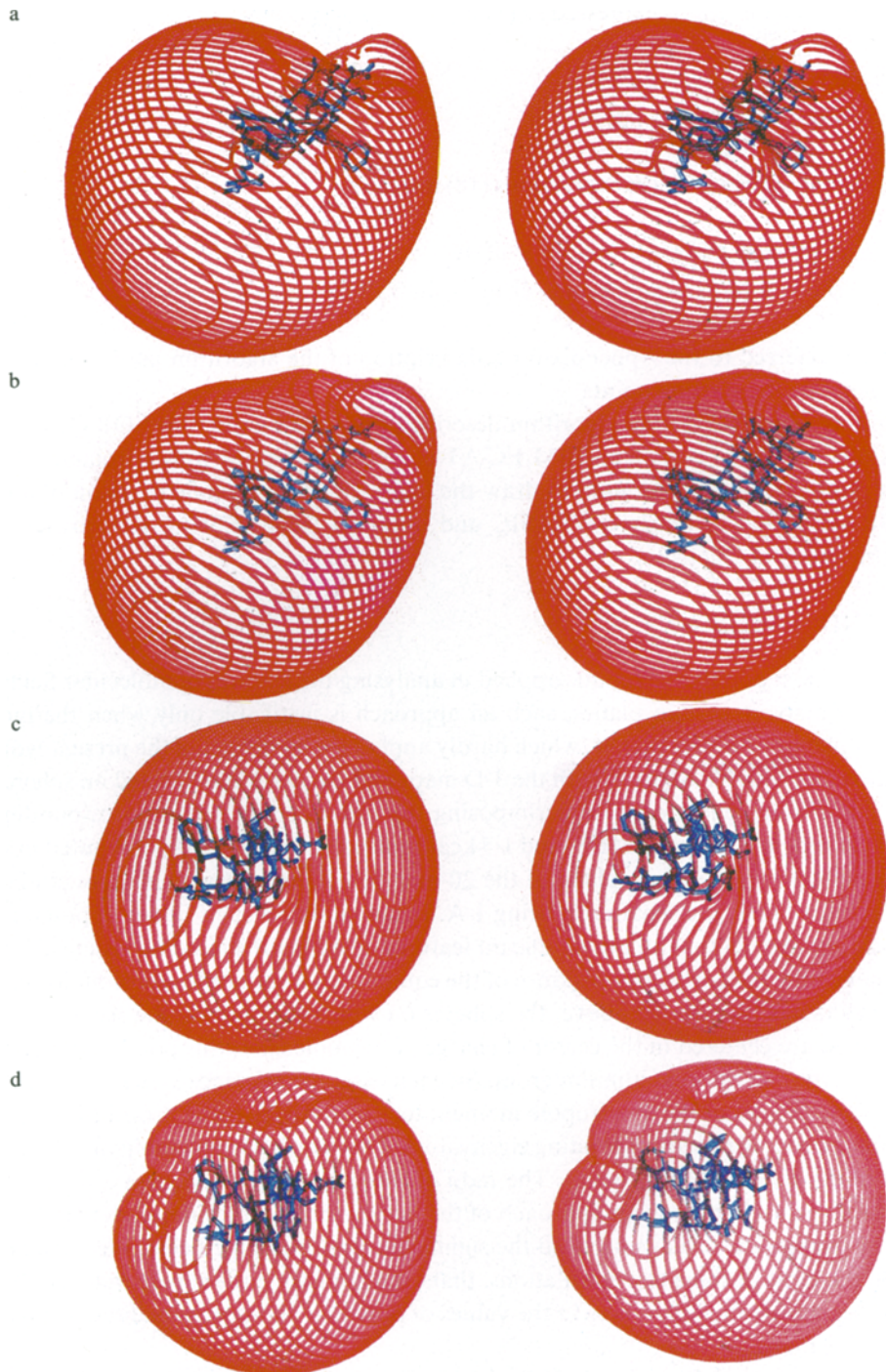


Fig. 5. The 3-D maps of MEP and MEF (red) of two low-energy conformations of [Ths¹]-AVP shown together with the molecules (blue). The value of MEP of the shapes presented is 20 kcal/mol and that of MEF 1.5 kcal/mol. Parts (a)–(d) as in Fig. 3.

In the case of the plane this is expressed as (17):

$$\begin{aligned}\delta f/\delta\varphi &= u_1\delta f/\delta x + u_2\delta f/\delta y + u_3\delta f/\delta z \\ \delta f/\delta\psi &= v_1\delta f/\delta x + v_2\delta f/\delta y + v_3\delta f/\delta z\end{aligned}\quad (17)$$

In the case of the sphere we have expressions (18) instead:

$$\begin{aligned}\delta f/\delta\varphi &= -\sin\varphi\sin\psi\delta f/\delta x + \cos\varphi\sin\psi\delta f/\delta y \\ \delta f/\delta\psi &= \cos\varphi\cos\psi\delta f/\delta x + \sin\varphi\sin\psi\delta f/\delta y - \sin\psi\delta f/\delta z\end{aligned}\quad (18)$$

The reader is referred to the Appendix for a description of the algorithm used to solve system (15) and to generate the starting points.

The programs which realise the algorithm described have been written in FORTRAN 77. All the calculations have been run on an IBM PC AT computer equipped with a Roland DG DXY 880 A color plotter. The software used to draw the figures was our modified version of a BASIC program GRAFSTER run under GWBASIC and obtained from M.Sc. J. Kostrowicki of the Technical University of Gdańsk.

RESULTS AND DISCUSSION

Although the most popular technique applied in analysing the features of molecular fields is the construction of maps in certain planes, such an approach is justifiable only when the molecule under study is planar or nearly planar, which hardly applies to the subject of the present work. We thought it therefore suitable to begin with the 3-D maps and the maps constructed on spheres.

The 3-D maps were generated by superimposing the equipotential curves corresponding to a value of 20 kcal/mol in the case of MEP, and 1.5 kcal/mol in the case of MEF, computed in several planes perpendicular to the mean plane of the 20-membered ring of the analogues studied and stacking over each other, the separation being 1 Å. In the choice of such values of potentials, we took into account the fact that all the significant features of the fields should be visualised, preserving at the same time the fairly large distance of the equipotential surface from the molecule under consideration. As has been stated above, the spheres on which the maps of the second type have been constructed are centered in the center of charge of the molecules, this point being very close to the central carbon of the guanidinium group. In each case, the reference system was chosen according to the main axes of the quadrupole moment tensor, the axes being arranged with respect to the ascending order of the corresponding eigenvalues. This freed us from ambiguity in the choice of the basis of the spherical coordinates. The radii of the spheres were assigned a value of 20 Å, which provides against too close an approach of the curves to the molecules under study, and at the same time enables the visualising of all the significant features of the fields. We have however observed, on the basis of some test calculations, that even increasing the sphere radius to 35 Å results only in decreasing the differences in the values of potential and not in qualitative changes of the pattern of the maps.

The stereoviews of the 3-D maps of MEP and MEF for all the analogues studied in their two low-energy conformations, of T_2^- (lower in energy) and C_1^+ (higher in energy) shape, respectively, according to the classification of our previous paper [17] are shown in Figs. 3a-d to 5a-d, together

with the molecules which are embedded in the equipotential surfaces. To make things clearer the stereoviews of the compounds studied are displayed in Fig. 6a–f.

A common feature of all the maps is their nearly spherical shape in the region of space facing the charged guanidinium group, a point which is easy to understand, because facing this group both MEP and MEF behave as the fields of a single point charge. Significant deviations from the spherical field emerge only in the regions of space where other parts of a molecule are pronounced. At this point substantial differences can be observed between the T_2^- - and C_1^+ -shaped conformations. The second is more compact and therefore generates fields of shape resembling a slightly compressed ball with few characteristic features. In contrast to this, the fields of the more stretched T_2^- -shaped conformation exhibit significant protrusions in the region of space surrounding glutamine and asparagine. On the other hand, close to these regions are significant holes in the field surfaces, which can be attributed to lowering the field.

Similar conclusions can be drawn when analysing the maps on spheres. Because in the case of C_1^+ -shaped conformation the differences between the maps corresponding to different analogues are negligible, the maps of MEP and MEF are shown only for [Mpa¹]-AVP (Fig. 7a–d). In the case of [Cpp¹]-AVP and that of [Ths¹]-AVP only the maps corresponding to the T_2^- -shaped conformation are presented (Figs. 8a,b and 9a,b). All the maps mentioned are presented in polar coordinates. To illustrate the location of the maxima and minima observed in the maps with respect to the molecules, example stereoviews of a few curves of the maps of MEP of [Mpa¹]-AVP after conversion into the Cartesian coordinates (cf. Eqs. 13), together with the molecules are shown in Fig. 8.

As revealed in Figs. 7b,c and 10b, the C_1^+ -shaped conformation exhibits a broad zone of high MEP and MEF which almost surrounds the plane containing the guanidinium group. In this zone there are several windows surrounding the regions of higher potential which approximately coincide with the directions of the guanidinium protons, with the exception of one which faces the glutamine protons. Thus, there are no greater deviations from the field which would be generated by a separate guanidinium group. In the case of the T_2^- -shaped conformation, in contrast, the field of the guanidinium group is significantly perturbed. The bumps and holes exhibited in the 3-D maps are reflected as curves surrounding the areas of high and low potential, respectively (Figs. 7a,b, 8a,b, 9a,b and 10a).

To make the picture more complete, maps of MEP and MEF of [Mpa¹]-AVP in its T_2^- -shaped conformation constructed in a plane which is parallel to the mean plane of the 20-membered ring and intersects asparagine and tyrosine side chains, being also very close to the side chain of glutamine, are displayed in Fig. 11a,b. Neither the maps of the C_1^+ -shaped conformation nor those of other analogues are shown, as all the differences are quite well visualised in both 3-D maps and maps on the spheres. As is shown, a characteristic feature of the maps is that at sufficiently large distances there is only one equipotential curve corresponding to a given value of potential. It can also be observed that the greater the distance, the more the curves resemble circles. This is evident because the system under study is charged due to the presence of the guanidinium group and its electrostatic potential tends to the potential of a single point charge when increasing the distance from the molecule.

Because there are substantial differences between the fields generated by the molecules in their T_2^- - and C_1^+ -shaped conformations, the detailed discussion below is divided into the parts corresponding to the types of conformation.

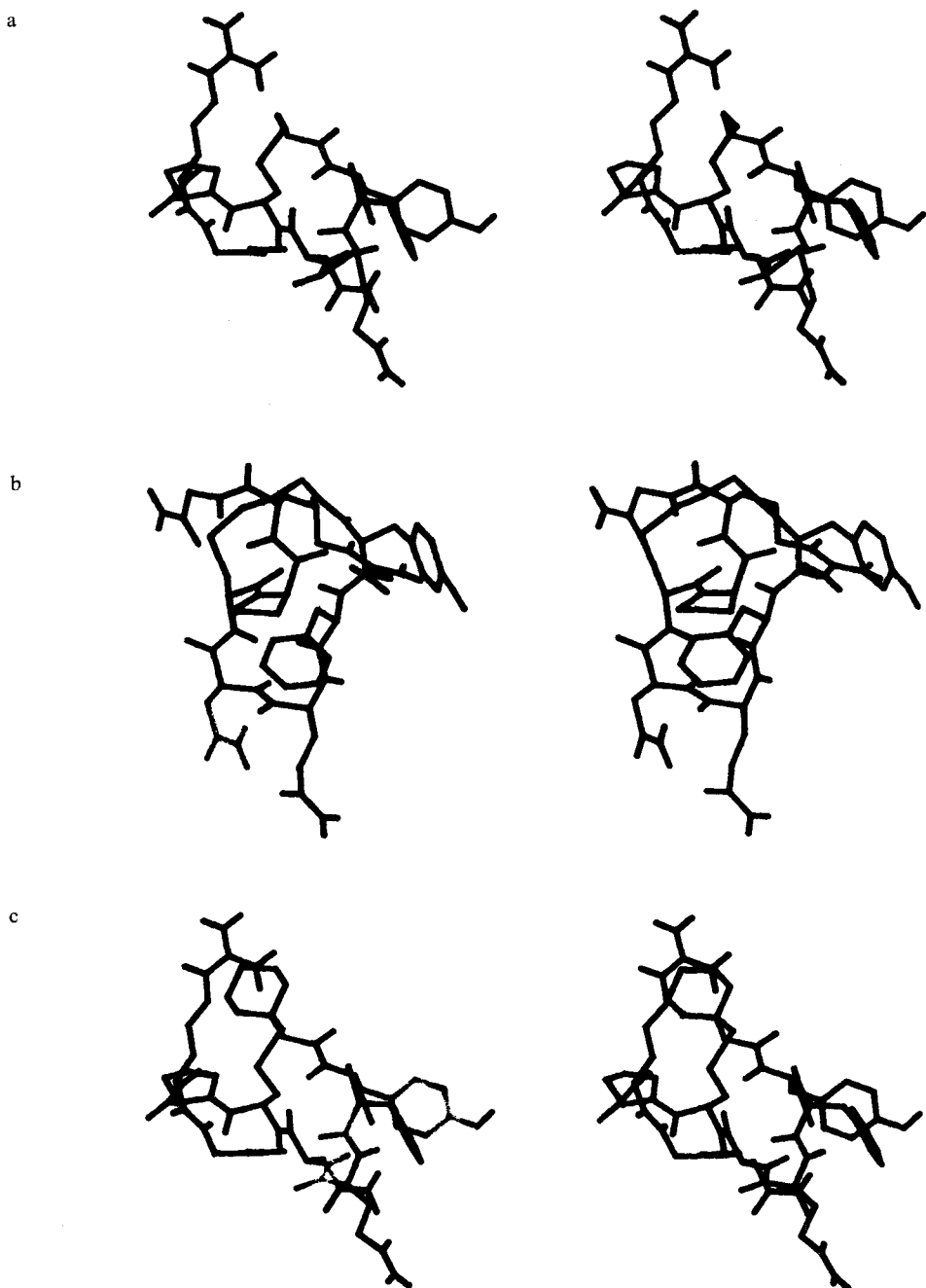
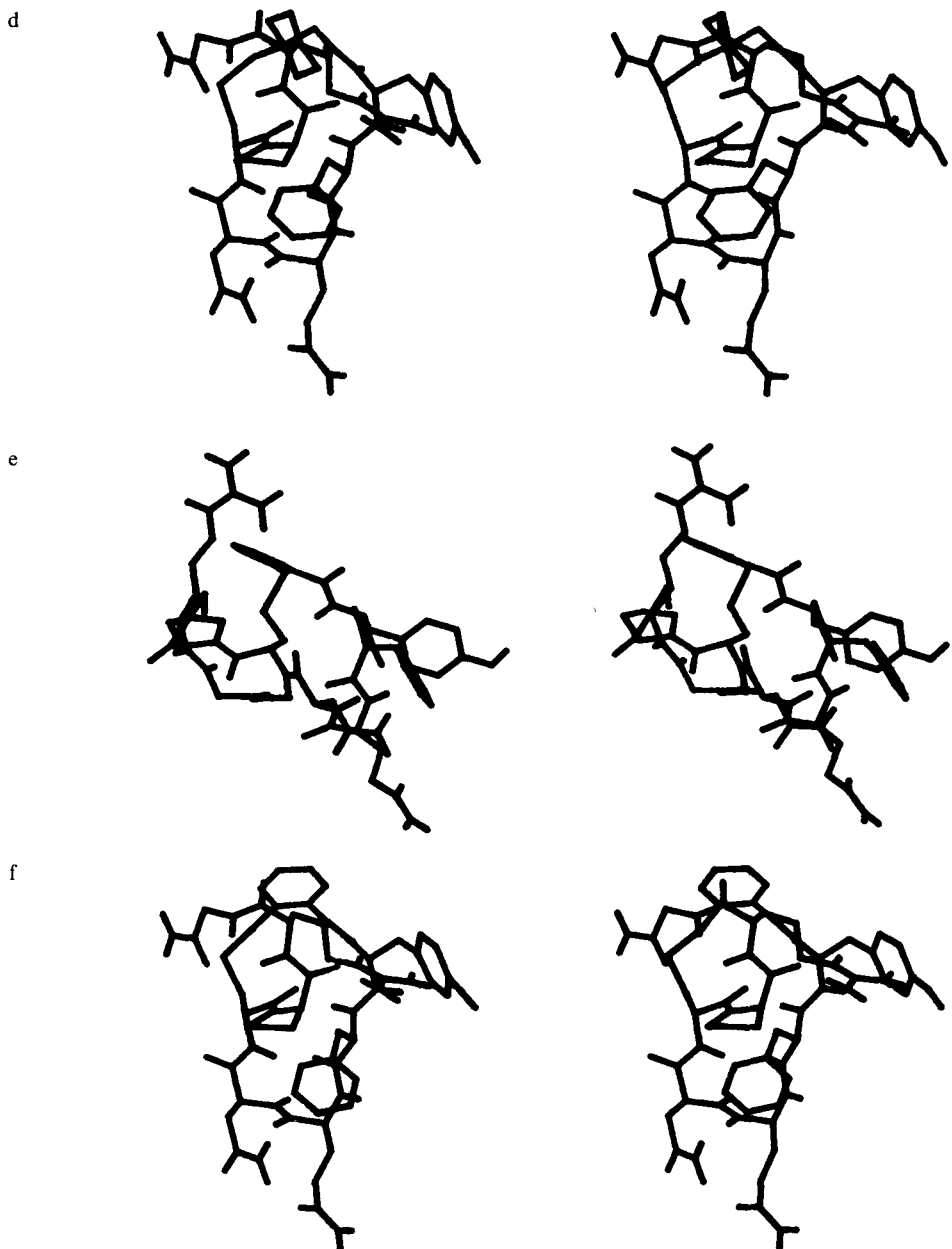


Fig. 6. Stereoviews of the compounds studied projected onto the mean planes of the 20-membered ring: (a) $[Mpa^1]$ -AVP, T_2^- -shaped conformation; (b) $[Mpa^1]$ -AVP, C_1^+ -shaped conformation; (c) $[Cpp^1]$ -AVP, T_2^- -shaped conformation; (d) $[Cpp^1]$ -AVP, C_1^+ -shaped conformation; (e) $[Ths^1]$ -AVP, T_2^- -shaped conformation; (f) $[Ths^1]$ -AVP, C_1^+ -shaped conformation.



The case of T_2^- -shaped conformation

As has been mentioned above, a common feature of both MEP and MEF is the significant protrusion in the region surrounding the glutamine side chain, which can be attributed to the amide protons. A smaller bump is also observed near the C-terminal glycine. On inspection of the maps, a region of slightly higher potential on the spheres can be found around the guanidinium > NH

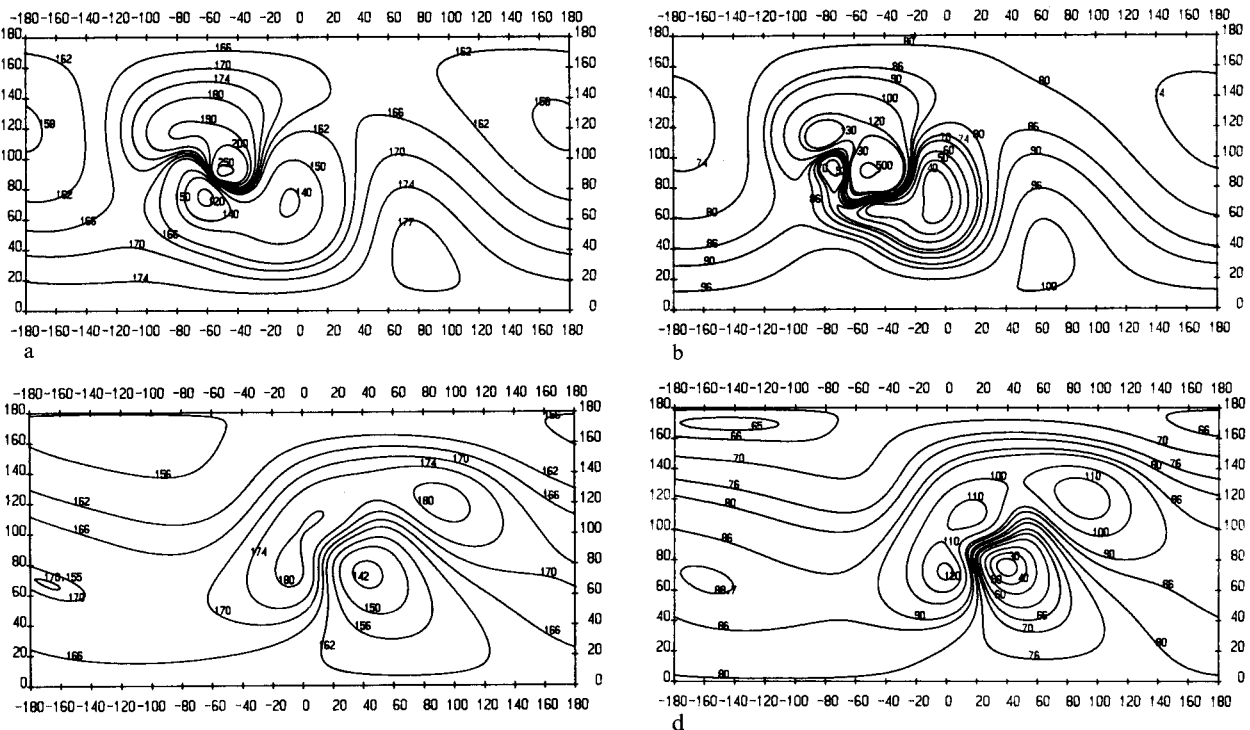


Fig. 7. Maps of MEP and MEF of $[Mpa^{-1}]$ -AVP in its two low-energy conformations (T_2^- - and C_1^+ -shaped, respectively) constructed on the spheres centered in the charge center of the molecule and of radius 20 Å in the polar coordinates. The values of MEP (in kcal/mol) are multiplied by 10 and those of MEF by 100. (a) T_2^- shaped conformation, MEP; (b) T_2^- shaped conformation, MEF; (c) C_1^+ shaped conformation, MEP; (d) C_1^+ shaped conformation, MEF.

proton; surprisingly, in a region of the sphere which should be influenced mostly by the guanidinium group, there is a slight decrease in the fields. This on closer examination seems to be due to the presence of the negatively charged lone pairs of the disulphide bridge (not shown in the figures for the sake of clarity). It can also be noted that these features are too weak to be reflected in the 3-D maps presented.

Regardless of the similarities presented between MEP and MEF, there are also substantial differences of which the most marked are those near the side chains of tyrosine and asparagine. Due to the presence of the negative hydroxyl oxygen which is exposed outside, MEP is substantially lowered near the side chain of tyrosine (see Figs. 7a and 11a). However, from inspection of the map shown in Fig. 11a, a significant concentration of the equipotential lines can be observed near the tyrosine hydroxyl which results in a high electrostatic field. This appears as a significant bump in the 3-D maps (Figs. 3b, 4b, and 5b), or as an additional region of high MEF in the maps on the spheres (Figs. 7b, 8b, and 9b), and can also be observed in the map constructed in the plane chosen (Fig. 11b). The same applies to the region of the side chain of asparagine. Because its outermost amide proton is hydrogen-bonded to the glutamine side chain carbonyl oxygen, the exposed carbonyl oxygen of the asparagine side chain generates a negative contribution to MEP which is reflected as a bump of low potential buried inside the surfaces of higher potential (Fig. 11a).

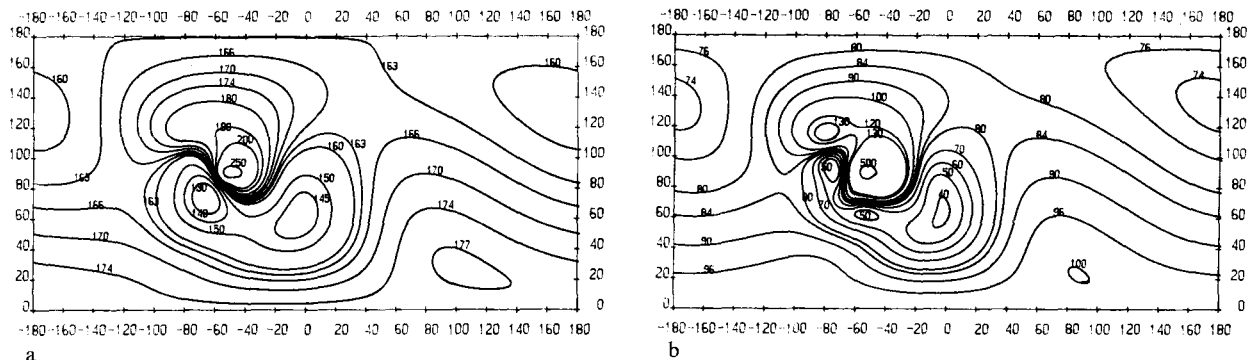


Fig. 8. Maps of MEP (a) and MEF (b) of [Cpp¹]-AVP in its lowest energy (T_2^- -shaped) conformation constructed on the spheres centered in the charge center of the molecule and of radius 20 Å in the polar coordinates. The values of MEP (in kcal/mol) are multiplied by 10 and those of MEF by 100.

In the 3-D map of MEF, a deep depression can be observed between the bumps generated by glutamine, tyrosine, and the asparagine side chains which is due to the presence of a hydrogen bond between the side chains of glutamine and asparagine. In the maps on the spheres it is reflected as a region of low potential located between the high-potential regions of the groups mentioned. Another pronounced region of low potential faces the backbone of Gly⁹ and Pro⁷.

Generally speaking, from the maps on the spheres it can be concluded that a very characteristic feature of the fields are two kidney-shaped regions matching each other and enclosing the areas of particularly high and particularly low potential, respectively (see Figs. 7a,b, 8a,b, 9a,b, and 10a). In the case of [Mpa¹]-AVP and [Cpp¹]-AVP these regions have an almost identical shape. In contrast, as shown in Fig. 9a,b, in the case of [Ths¹]-AVP their shape is different in some details. First, the positions of these regions in the spherical coordinates are different when compared with the former analogues, which means that the main axes of the molecular quadrupole are differently oriented with respect to the molecule. Although after converting the curves into the Cartesian coordinates the maps become more similar, the region of the lowest MEP and MEF in the case of

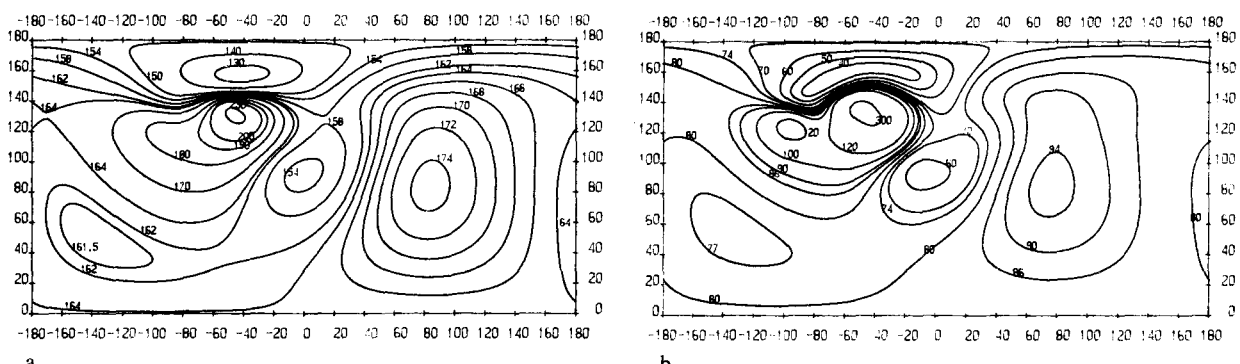


Fig. 9. Maps of MEP (a) and MEF (b) of [Ths¹]-AVP in its lowest energy (T_2^- -shaped) conformation constructed on the spheres centered in the charge center of the molecule and of radius 20 Å in the polar coordinates. The values of MEP (in kcal/mol) are multiplied by 10 and those of MEF by 100.

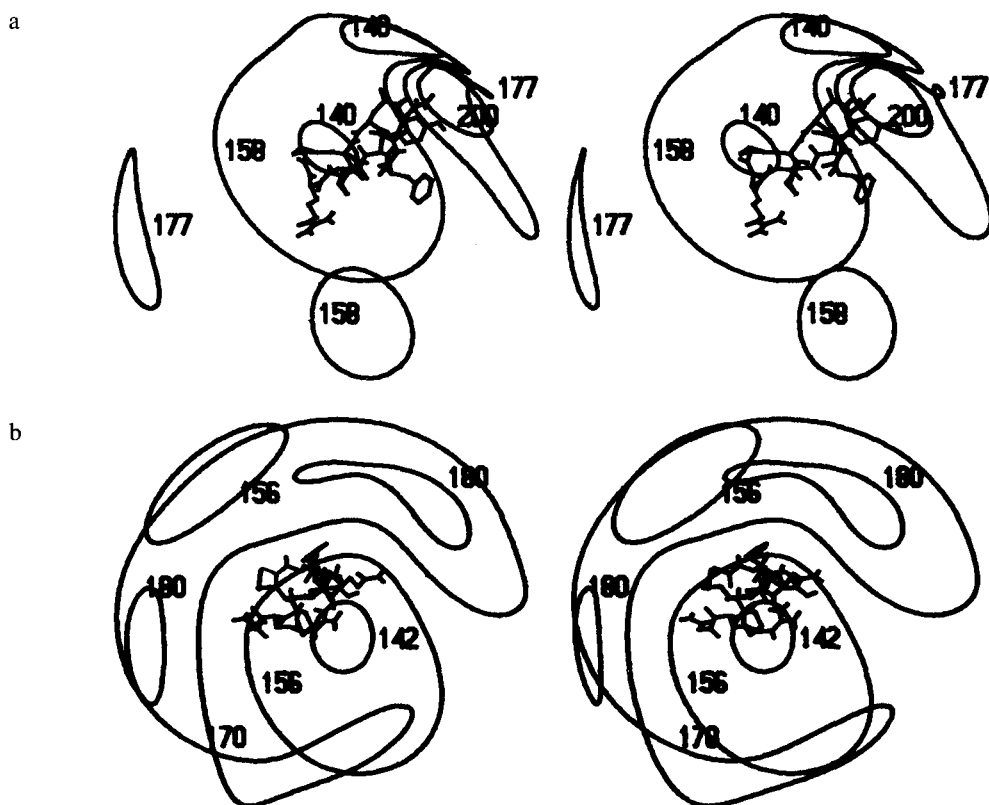


Fig. 10. Example stereoviews of the maps of MEP of Fig. 7 after conversion into the Cartesian coordinates.

[Ths¹]-AVP appears near Asn⁵ and Tyr² side chains, and is broader than the corresponding region in the case of [Mpa¹]-AVP and [Cpp¹]-AVP, while the region near Pro⁷ and Gly⁹ backbones has a potential not as low as that of the other two analogues. In the 3-D maps these differences are reflected as enhancing both the depression, which overlooks the 20-membered ring and begins approximately at the asparagine side chain, and the small bump near the glutamine, as far as the fusion of it with the rest of the surface in the case of MEP. A general conclusion which can be drawn from the comparison of the maps of [Ths¹]-AVP with those of [Mpa¹]-AVP and [Cpp¹]-AVP is that the fields of the first are significantly less 'steep' than those of the latter.

Inspection of the maps of MEF in planes reveals that this field is high and vanishes on increasing the distance comparatively slowly in the regions of space where the contribution from the guanidinium group dominates, and very much decreases on increasing the distance in the regions where the protrusions in the 3-D maps can be observed. It can therefore be predicted that nonspecific solvation is likely to occur around the guanidinium group, while the parts of the molecule where the field strongly differs from the spherical one are freer owing to the thermal motion. Thus the shape of MEP and MEF in the last-mentioned regions are probably recognised by the receptor. This is confirmed by the fact that the presence of asparagine in the 5th position, which belongs to the part of the molecule generating the peculiarities of the field, is essential for the biological ac-

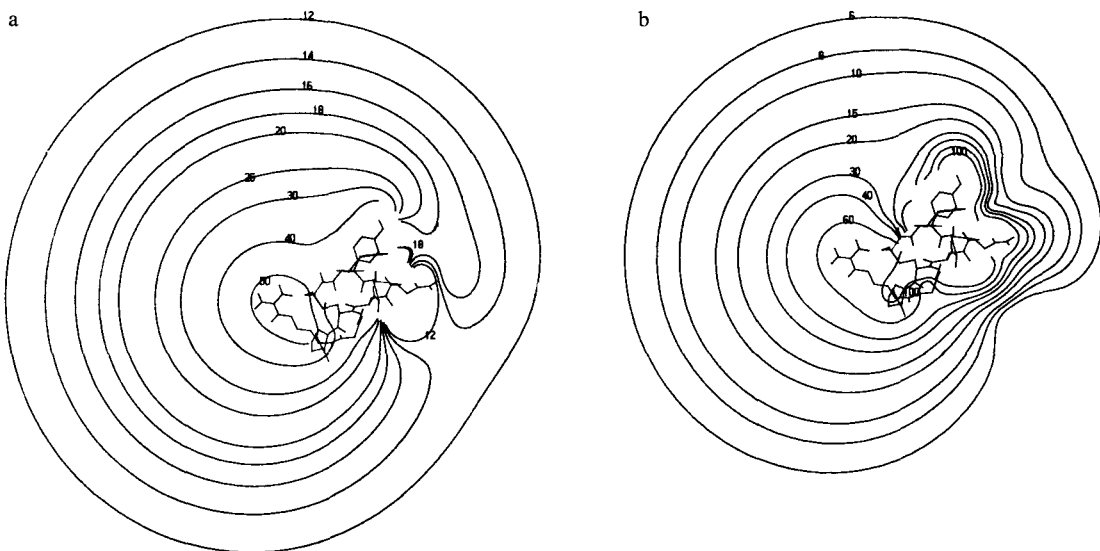


Fig. 11. Example maps of MEP (a) and MEF (b) of $[Mpa^1]$ -AVP in its lowest energy (T_2^- -shaped) conformation constructed in a plane parallel to the mean plane of the 20-membered ring which intersects the asparagine and tyrosine side chains and is very close to the glutamine side chain. The values of MEP and MEF are in kcal/mol, those of MEF are multiplied by 10.

tivity of the vasopressin and oxytocin derivatives [31], and by very weak agonistic activity in the case of $[Ths^1]$ -AVP whose field is different in these regions. However, to justify this conclusion the harmonic deviations from the minimum-energy geometry at least should be taken into account to allow the calculation, by means of statistical mechanics (the Z-approximation [32]), of the 'average' field corresponding to the neighbourhood of a conformation.

The case of C_1^+ -shaped conformation

Contrary to the T_2^- -shaped conformation, in this case there are no substantial differences between the analogues. As was mentioned above, the fields are nearly spherical, with some regions of depression. Only the 3-D maps of MEF exhibit a weak protrusion around the glutamine amide side-chain protons. Because the tyrosine hydroxyl is hydrogen-bonded to the guanidinium group, its contribution to the MEP and MEF is buried in the positive field of guanidinium. The most significant difference between MEP and MEF is that, in the first case there is a hole in the 3-D surface facing Gln^4 and Asn^5 , while in the second case it is shifted to face the region of the backbones of Tyr^2 and Phe^3 . In the case of MEP there is also a smaller surface of the potential of 20 kcal/mol buried inside the main surface, which appears at the sulphur of the first residue. It can also be noted that the hydrogen bond between the side chains of Gln^4 and Asn^5 is also reflected in MEF as a depression in the 3-D maps, and as a region of small potential in the maps on the spheres.

Because both MEP and MEF are little featured in the case of the C_1^+ conformation and, moreover, there are almost no differences between the active and inactive analogues, it can be concluded that this type of conformation is probably not the one which is recognised by the receptor.

CONCLUSIONS

The results presented have shown that the differences in the biological activity of the compounds studied correlate with the differences in the shape of their MEP and MEF, even if their conformations are assumed to be almost the same. Obviously, the conformational calculations presented in our previous paper [17] are not a global analysis of the problem, and it may therefore appear that [Ths¹]-AVP in fact has quite different conformational space available. On the other hand, the lack of activity of [Ths¹]-AVP may be simply due to the steric hindrance (a planar benzene ring) which does not allow for binding, while the cyclohexane ring in position 1 in the case of [Cpp¹]-AVP need not be a sufficient hindrance to prohibit this process. It is important to note that the T₂⁻-shaped conformation, which generates the most featured fields with the protrusions near the regions presumed to be responsible for the biological activity, is very similar to the cooperative model of vasopressin, in particular in the geometry of the 20-membered ring and in the property that the side chains of tyrosine, glutamine, asparagine and arginine (lysine in the case of [Lys⁸]-AVP) are exposed outside the molecule.

Finally, it can be noted that the postulated responsibility of the protrusions in MEP and MEF near the glutamine and asparagine side chains is in agreement with the influence of the substitutions in positions 4 and 5 on biological activity in the series of oxytocin and vasopressin analogues [33]. Replacing the carboxyamide of asparagine by any other group results in almost complete loss of both agonistic and antagonistic activity, which means that it is directly involved in binding. However, there is also some influence of the substitution in position 4. Replacing glutamine by the glutamic acid whose side-chain carboxyl must occur in the anionic form in physiological conditions results in the case of oxytocin agonists in almost complete loss of activity (the [Glu⁴]-AVP analogue has not been synthesized as yet). From the point of view of recognition via the MEP and/or MEF this is evident, because in such a case the shapes of these fields near the asparagine side chain will change substantially due to the presence of a negative group. On the other hand, the conservation of activity on replacing the glutamine side chain by a nonpolar group is also easy to explain, as both the MEP and the MEF of a single asparagine are presumably similar to the combined fields of both asparagine and glutamine. The loss of activity on replacing L-Gln by D-Gln, if it is not due to substantial changes in the conformational space available, can be explained in such a case by the presence of two separate bumps due to glutamine and asparagine, respectively.

The remarkable decrease of the biological activity on methylation of the carboxyamide group of glutamine can also now be explained, though not in terms of the field. Let us note that in both conformations studied, there is a hydrogen bond between the side chains of these residues which involves the glutamine carbonyl oxygen and one of the asparagine amide protons. This causes a very close approach of both groups and may be the reason that any steric hindrance introduced is so important.

There is no doubt that to get a more complete picture of the features of MEP and MEF responsible for recognition, more analogues should be compared and, first of all, the conformational space of at least the most rigid 20-membered ring of vasopressin should be analysed more thoroughly. Moreover, to enable a better comparison of the fields to be carried out the Z-approximation, at least, should be applied. Work on this is now in progress in our laboratory. However, even the present results are promising and can easily be correlated with experiment.

Our final remark is that the three types of maps used to analyse the fields are fully complementary. The 3-D maps are the most communicative, though not all the features of a field can be displayed at a time. More information is provided by the maps constructed on the spheres, though they are not as informative and sometimes difficult to read properly. Finally, the maps constructed in certain planes which may be chosen after looking at the former types of maps are both communicative and carry a maximal amount of information as far as the planes chosen are concerned (for example, about the concentration or depletion of the field under study).

ADDENDUM

Very recently, a new method for analysing the topographic properties of the 3-D surfaces of MEP has been worked out by Dean et al. [34]. This method makes it possible to compare the electrostatic potential field of dissimilar molecules and is, to some extent, similar to our analysis of the maps of the fields constructed on the spheres.

ACKNOWLEDGEMENTS

This work was supported by grants CPBR-3.13.4.3.2 and CPBP-05.06.1.5.4. The authors thank M.Sc. J. Kostrowicki of the Technical University of Gdańsk, for the program GRAFSTER.

APPENDIX

In the numerical solution of system (15) two problems are to be encountered: (i) the choice of the method of numerical integration, and (ii) the choice of the starting points (ϕ°, ψ°) .

Let us first consider problem (i). Obviously, many well-known methods of integrating the systems of ordinary differential equations can be applied here; for example, the Runge-Kutta methods [35]. In our special case, however, it is recommended that use be made of the fact that the solution of the system describes a curve $f(\phi, \psi) = \text{const.}$, and therefore each infinitesimal move along this curve is at the same time a move across the gradient of f in the (ϕ, ψ) space. This implies the following concept: in order to obtain the next point of the curve under consideration, move a little from the current one across the gradient and then, having obtained a point which is a bit outside the curve, move along the gradient until the curve is met. This is illustrated in Fig. 12.

The following equations describe the changes in ϕ and ψ at the first step:

$$\begin{aligned}\phi^{i+1, 1} &= \phi^i + \delta\phi/\delta t \Delta t \\ \psi^{i+1, 1} &= \psi^i + \delta\psi/\delta t \Delta t\end{aligned}\tag{19}$$

where $\phi^i = \phi(t^i)$, $\psi^i = \psi(t^i)$, $t^i = t^\circ + i\Delta t$, $\delta\phi/\delta t$ and $\delta\psi/\delta t$ are defined by (15), and Δt is the step of integration; we used 0.5 \AA in the case of the maps in planes and 1° in the case of the maps on spheres.

It can easily be observed that the equations above are simply one-step Euler formulae [35]. The second step may be achieved by Newton's method [36]. The derivation of the iteration formula is as follows:

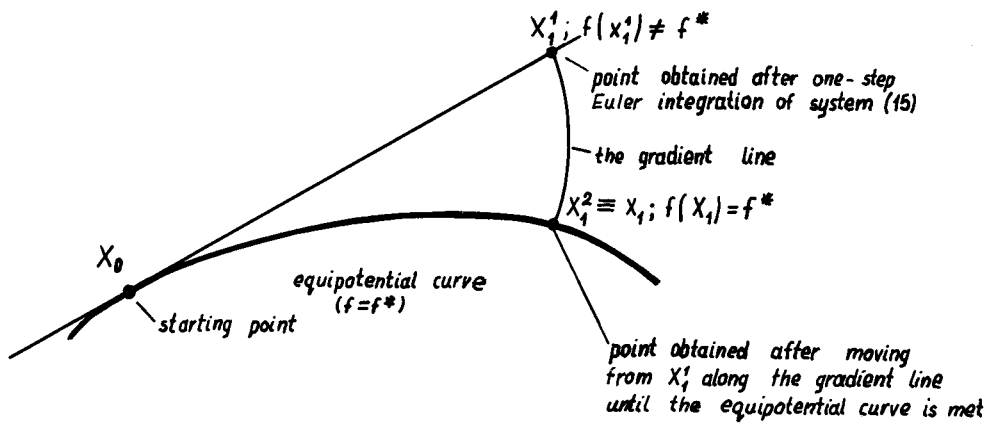


Fig. 12. Schematic representation of the method of numerical integration used.

Assuming that τ is a variable describing the movement along the gradient, the values of φ and ψ in $p + 1$ th iteration connected with the corresponding changes in τ are given by (20):

$$\begin{aligned}\varphi^{(p+1)} &= \varphi^{(p)} + (\delta\varphi/\delta\tau)^{(p)} \Delta\tau^{(p)} \\ \psi^{(p+1)} &= \psi^{(p)} + (\delta\psi/\delta\tau)^{(p)} \Delta\tau^{(p)}\end{aligned}\quad (20)$$

Because the movement is along the gradient we have (21):

$$\begin{aligned}\delta\varphi/\delta\tau &= \delta f/\delta\varphi \\ \delta\psi/\delta\tau &= \delta f/\delta\psi\end{aligned}\quad (21)$$

The Newton iteration formula for the increment in τ in p th iteration is given by (22);

$$\Delta\tau^{(p)} = [(\delta f/\delta\tau)^{(p)}]^{-1} (f^* - f(\tau^{(p)})) \quad (22)$$

with

$$\delta f/\delta\tau = \delta f/\delta\varphi \delta\varphi/\delta\tau + \delta f/\delta\psi \delta\psi/\delta\tau = (\delta f/\delta\varphi)^2 + (\delta f/\delta\psi)^2$$

where f^* denotes the required function value.

Substituting $\Delta\tau^{(p)}$ from (22) into (21) we obtain the final formula (23):

$$\begin{aligned}\varphi^{(p+1)} &= \varphi^{(p)} + w^{(p-1)}(\delta f/\delta\varphi)^{(p)} (f^* - f^{(p)}) \\ \psi^{(p+1)} &= \psi^{(p)} + w^{(p-1)}(\delta f/\delta\psi)^{(p)} (f^* - f^{(p)})\end{aligned}\quad (23)$$

where

$$w = (\delta f/\delta\varphi)^2 + (\delta f/\delta\psi)^2$$

Iteration stops when $|f^{(p)} - f^*|$ is less than the required tolerance, in this work equal to 0.0001 kcal/mol. After this we obtain the required point $\varphi^{i+1, 2}, \psi^{i+1, 2}$.

Obviously, the question of when to stop integrating is still to be answered. In our algorithm there are the following criteria:

(1) The distance between the first and the current point of the curve and the difference between the gradients of f computed at these points are less than certain critical values, which means that the curve has been closed. We used half a value of the integration step in the case of the first criterion, and 0.1–0.5 kcal/Å (kcal/deg) in the case of the second.

(2) The current point is outside the specified region (i.e., $\varphi > \varphi_{\max}$ or $\varphi < \varphi_{\min}$ or $\psi > \psi_{\max}$ or $\psi < \psi_{\min}$).

(3) The distance of the current point (after converting it into the Cartesian coordinates) from the nearest atom of the molecule is less than a critical value (2 Å, in our case).

In the two last cases, integration is started again from the first point of the curve, but the opposite direction is taken.

We have found that the above procedure of numerical integration is a very effective one. Owing to the quadratic convergence of Newton's method in practice, only two to four iterations are required to improve the point obtained in the first (Euler) step.

Let us now turn to the problem of choosing the starting points (φ^*, ψ^*) . This is a very important task indeed, because it often happens that there is more than one curve of a certain value of f . In our algorithm the region in which the curves are calculated is a certain rectangle in the (φ, ψ) space. On such a rectangle we define a net whose steps are (S_φ, S_ψ) . Then iteration over $\varphi_i := \varphi_0 + iS_\varphi$, $i = 0, 1, \dots, n_\varphi$ is performed. At each step for each point (φ_i, ψ_j) , where $\psi_j = \psi_0 + jS_\psi$, $j = 0, 1, \dots, n_\psi$ the value of $f(\varphi_i, \psi_j) = f_{ij}$ is calculated. Then a pair of indices j and $j+1$ is sought, for which either $f_{ij} \leq f^*$ and $f_{i, j-1} \geq f^*$ or $f_{ij} \geq f^*$ and $f_{i, j-1} \leq f^*$ holds. When at least one such pair is found, linear interpolation is performed between ψ_j and ψ_{j+1} in order to find such $\psi_j \leq \psi_j^* \leq \psi_{j+1}$ that $f(\varphi_i, \psi_j^*) \equiv f_{ij}^* \approx f^*$ (in the first-order approximation). This leads to the following interpolation formula:

$$\psi_j^* = \psi_j + \frac{\psi_{j+1} - \psi_j}{f_{i, j+1} - f_{ij}} (f^* - f_{ij}) \quad (24)$$

The value of ψ_j^* is then adjusted by means of the secant method [37].

The above procedure gives an array of values, ψ_{ij}^* , each of which can be used as a starting point for numerical integration. Provided that the net is dense enough, no curve may be omitted. On the other hand, making the net too dense is not recommended either, as this unnecessarily enlarges the computational effort. In practice we have found that a step length of 5 Å is sufficient in the case of the maps in planes and 10° for those on spheres. This gives a very small number of points when compared to that required for the procedure of constructing the curves by interpolating between the points of the net.

The method of using the starting points obtained is as follows: beginning from $i = 0, j = 0$ consider the subsequent (φ_i^*, ψ_j^*) . From each such point, start the integration. At each step of integration check whether there is such a pair of indices, λ and μ that the curve has in this step intersected a segment defined by $\varphi = \varphi_\lambda$, $\psi_\mu \leq \psi \leq \psi_{\mu+1}$. If so, check if any $\psi_{\lambda j}^*$ is within this segment and eliminate it from the set of the starting point in such a case. Having completed integration (according to the stop criteria given above) turn to the next starting points, or stop if all of them have been examined.

REFERENCES

- 1 Lehninger, A.L., Biochemistry (German edition), Verlag Chemie, Weinheim, 1979, pp. 661–662.
- 2 Hruby, V.J. and Lebl, M., In Jošt, K., Lebl, M. and Brtník, F. (Eds.) CRC Handbook of Neurohypophyseal Hormone Analogs, Vol. 1, Part 1, CRC Press, Boca Raton, 1987, pp. 106–107.
- 3 Gazis, D., In Jošt, K., Lebl, M. and Brtník, F. (Eds.) CRC Handbook of Neurohypophyseal Hormone Analogs, Vol. 1, Part 2, CRC Press, Boca Raton, 1987, pp. 51–63.
- 4 Lehninger, A.L., Biochemistry (German edition), Verlag Chemie, Weinheim, 1979, pp. 662–675.
- 5 Balodis, Yu.Yu., Nikiforovich, G.V., Grinsteine, I.V., Vegner, R.E. and Chipens, G.I., FEBS Letters, 86 (1978) 239–242.
- 6 Balodis, Yu.Yu. and Nikiforovich, G.V., Bioorg. Khim., 6 (1980) 865–875.
- 7 Hagler, A.T., In Hruby, V.J. (Ed.) The Peptides, Vol. 7, Academic Press, Orlando, 1985, pp. 213–299.
- 8 Paine, G.H. and Scheraga, H.A., Biopolymers, 24 (1987) 1391–1436.
- 9 Zimmerman, S.S., In Hruby, V.J., The Peptides, Vol. 7, Academic Press, Orlando, 1985, p. 205.
- 10 Némethy, K., Hodes, Z.I. and Scheraga, H.A., Proc. Natl. Acad. Sci. U.S.A., 75 (1978) 5760–5764.
- 11 Weiner, S.J., Kollman, P.A., David, A.C., Chandra Singh, U., Ghio, C., Alagona, G., Profeta, S. and Weiner, P., J. Am. Chem. Soc., 106 (1984) 765–784.
- 12 Hall, L.H. and Kier, L.B., J. Theoret. Biol., 58 (1976) 177–195.
- 13 Walter, D.E. and Hopfinger, A.J., In Kuchar, M. (Ed.) QSAR in Design of Bioactive Compounds, J.R. Prous, Barcelona, 1985, pp. 279–286.
- 14 Lee, R.H. and Rose, G.D., Biopolymers, 24 (1985) 1613–1627.
- 15 Goodford, P.J., J. Med. Chem., 28 (1985) 849–857.
- 16 Upton, R. and Gasking, H., Int. Lab. 9 (1988) 24–28.
- 17 Liwo, A., Tempczyk, A. and Grzonka, Z., J. Comput.-Aided Mol. Design, 2 (1988) 281–309.
- 18 Manning, M., Balaspiri, L., Moehring, J., Haldar, J. and Sawyer, W.H., J. Med. Chem., 19 (1976) 842–845.
- 19 Kruszyński, M., Lammek, B., Manning, M., Seto, J., Haldar, J. and Sawyer, W.H., J. Med. Chem., 23 (1980) 364–368.
- 20 Fahrenholz, F. and Grzonka, Z., unpublished results.
- 21 Grzonka, Z., Łankiewicz, L., Kasprzykowski, F., Liwo, A. and Melin, P., In Theodoropoulos, D. (Ed.) Peptides 1986, Walter de Gruyter, Berlin, 1987, pp. 493–496.
- 22 Schuster, P., In Schuster, P., Zundel, G. and Sandorfy, C. (Eds.) The Hydrogen Bond, Vol. 1, North Holland, Amsterdam, 1976, p. 71.
- 23 Jackson, J.D., Classical Electrodynamics (Polish edition), PWN, Warszawa, 1982, pp. 153–154.
- 24 Scrocco, E. and Tomasi, J., Top. Curr. Chem., 42 (1973) 95–170.
- 25 Hayes, D.M. and Kollman, P.A., J. Am. Chem. Soc., 98 (1976) 3335–3345.
- 26 Hadži, D., Hadošček, M., Kocjan, D., Šolmajer, T. and Avbelj, F., Croat. Chem. Acta, 54 (1984) 1065–1074.
- 27 Sanz, F., Manaut, F., Pascual, J.A. and Segura, J., In Boncza, G. (Ed.) WATOC '87, Abstracts, Magyar Kémikusok Egyesülete Készült, Budapest, 1987, p. 314, Abstract No. PB77.
- 28 Feynman, R.P., Leighton, R.B., Sands, M., The Feynman Lectures on Physics, Vol. 2 (Polish edition), PWN, Warszawa, 1971, pp. 188–189.
- 29 Ranghino, G., Clementi, E. and Romano, S., Biopolymers, 22 (1983) 1449–1460.
- 30 Singh, U.C. and Kollman, P., J. Comput. Chem., 5 (1984) 129–145.
- 31 Hruby, V.J. and Lebl, M., In Jošt, K., Lebl, M. and Brtník, F. (Eds.) CRC Handbook of Neurohypophyseal Hormone Analogs, Vol. 1, Part 2, CRC Press, Boca Raton, 1987, pp. 152–155.
- 32 Zimmerman, S.S., In Hruby, V.J., The Peptides, Vol. 7, Academic Press, Orlando, 1987, p. 195.
- 33 Jošt, K., In Jošt, K., Lebl, M. and Brtník, F. (Eds.) CRC Handbook of Neurohypophyseal Hormone Analogs, Vol. 1, Part 2, CRC Press, Boca Raton, 1987, pp. 156–159.
- 34 Dean, P.M., Callow, P. and Chen, P.L., J. Mol. Graph., 6 (1988) 28–34.
- 35 Williams, J., In Hall, G., and Whatt, J.M. (Eds.) Modern Numerical Methods for Ordinary Differential Equations, Clarendon Press, Oxford, 1976, pp. 2–19.
- 36 Ortega, J.M. and Rheinboldt, W.C., Iterative Solution of Nonlinear Equations in Several Variables, Academic Press, New York, 1970, pp. 180–188.
- 37 Ortega, J.M. and Rheinboldt, W.C. Iterative Solution of Nonlinear Equations in Several Variables, Academic Press, New York, 1970, p. 189.